FORMATION OF THE POROUS STRUCTURE OF BROWN COALS DURING CHEMICAL ACTIVATION AND ITS INFLUENCE ON BENZENE ADSORPTION

Aziza Abdikamalova[1], Izzat Eshmetov[1], Nozim Mamataliev[1], Alisher Kalbaev[1,2], Rasulbek Eshmetov[3], Bekzod Madaminov[3], Dilzoda Asqarova[4], Umidjon Raximov[4]

[1] **Institute of General and Inorganic Chemistry, Academy of Sciences of the Republic of Uzbekistan**, Tashkent 100170, Uzbekistan [2] **Karakalpak State University**, Nukus 230112, Uzbekistan [3] **Mamun University**, Khiva 220600, Uzbekistan [4] **Namangan State University of Technology**, Namangan 160115, Uzbekistan

ABSTRACT

In this study, a comprehensive investigation was carried out on the thermal and chemical modifications of brown coals of BPK and BR grades (Angren deposit, Uzbekistan) with the aim of establishing the regularities governing changes in their physicochemical and adsorption properties. Thermal analysis of the samples revealed the stages of carbon matrix degradation and the removal of volatile components. It was found that chemical activation leads to a significant decrease in the ash content of the coals, which is associated with the dissolution of mineral impurities during KOH treatment. Dispersion analysis demonstrated changes in particle size accompanied by increased structural fragmentation with higher KOH consumption, which was confirmed by morphological analysis using scanning electron microscopy (SEM). The samples after activation exhibited a substantial development of porosity, the formation of network-like structures, and the expansion of the channel system, indicating intensive etching of the carbon matrix. Particular attention was given to the study of the textural characteristics of the activated coals using the low-temperature nitrogen adsorption–desorption method. It was revealed that increasing the KOH ratio promotes a significant growth in the specific surface area (up to 1371.4 m^2/g) and the formation of a predominantly microporous structure in BR coals, whereas BPK coals demonstrate a more developed mesoporous system. It was determined that the variation in pore size exerts a decisive influence on benzene adsorption activity. Despite the high specific surface area of the activated coals, their sorption capacity for benzene does not always increase proportionally. This discrepancy is attributed to the peculiarities of the pore structure: BR coals are dominated by narrow micropores (7–12 Å), which ensure high adsorption capacity due to capillary condensation and molecular interactions, while BPK coals contain a higher proportion of pores in the range of 10–25 Å, which limits the retention of benzene molecules.

Keywords: brown coal, chemical activation, porous structure, specific surface area, surface morphology, low-temperature nitrogen adsorption, adsorption activity, benzene.

INTRODUCTION

Continuous technological advancement, human activity, and the increasing industrialization of the modern world are leading to a constant rise in air and water pollution levels. The main threats to soil and surface water are posed by contaminated domestic and industrial wastewater, the extensive use of chemicals, and the growing application of pesticides in agriculture [1, 2]. The deterioration of water quality is also associated with the insufficiency of natural self-purification processes [3]. This is a complex process influenced by many factors, such as temperature, light availability, and the quantity and type of pollutants introduced. Another pressing issue is the growing

population, urban development, and industrial progress, all of which significantly contribute to air pollution [4]. Vast amounts of gases released into the atmosphere originate from vehicle emissions and the consumption of fossil fuels, the volumes of which continue to increase each year [5].

Oil spills represent a serious environmental threat, recurrently caused by human error and negligence. These incidents can be either intentional or accidental, with examples including military actions and sabotage, as well as natural disasters such as hurricanes, earthquakes, and explosions [6]. Such events not only harm human and animal health but also result in significant losses of energy and valuable petroleum products [7, 8]. The importance of prompt and effective remediation of oil spills stems from their far-reaching impacts on the environment, economy, and public health. In this context, activated carbon stands out as one of the key materials for pollution mitigation due to its outstanding adsorption properties. The development and application of activated carbon for the removal of petroleum contaminants from water is becoming an increasingly important task in the search for effective materials to combat the environmental consequences of oil spills [9, 10].

Effective treatment of wastewater and gases is often achieved through the use of activated carbons, which serve not only as adsorbents but also as catalysts or catalyst supports [11, 12]. In addition, the modern world faces the challenge of managing agricultural waste generated in large volumes [13]. Such waste can be thermally or chemically processed to produce valuable products such as biofuels and biogas [14]. Furthermore, methods have been developed to minimize waste volumes by converting them into useful products, such as activated carbons [15–18].

Activated carbon has long been recognized as a highly effective adsorbent, widely used in various fields including wastewater treatment, air pollution control, and gas purification. The effectiveness of activated carbon is attributed to its high adsorption capacity, large surface area, and relatively low cost [1]. Activated carbon can be produced by various methods, including physical and chemical activation. Physical activation typically involves carbonization in an inert atmosphere or the use of steam, air, or CO_2 as activating agents [19–22]. Chemical activation involves the use of chemical reagents such as alkali metals [23], zinc chloride [24], and phosphoric acid [25] under inert conditions.

Alkaline activation of brown coal allows the production of activated carbon with a highly developed surface and excellent adsorption properties, making this method suitable for various carbon-containing materials [26-27]. The use of brown coal is advantageous due to the ability to achieve a significant specific surface area (up to 1400 m^2/g) with relatively small amounts of alkali (up to 1 g/g) [28, 29]. In contrast, for highly metamorphosed coals and anthracites, significantly larger amounts of alkali are required (up to 4 g/g for KOH and up to 7 g/g for LiOH) to achieve a specific surface area of up to 3000 m^2/g [30].

Low alkali/coal ratios, typical for brown coals, can result in poorly developed surfaces of activated carbon if insufficient alkali is used. However, high alkali usage is associated with increased costs and challenges in separating and disposing of the alkali after activation [30]. The economic efficiency of the process can be improved by optimizing the amount of alkali used, rather than selecting an expensive carbon precursor.

Studies on the activation of brown coal, such as Alexandrian brown coal, using alkali metal hydroxides (LiOH, NaOH, and KOH) have shown that the traditional sequence of impregnation and heating to 800°C in an inert atmosphere can be improved by replacing it with a thermal shock process. This approach increases the specific surface area to 1700 m^2/g and enhances the porous structure of the activated carbon [11-15]. This method

allows the production of activated carbon with a high yield (around 30%) and optimized properties for use in various applications, including air and water purification.

The aim of this study is to investigate BPK and BR grade brown coals from the Angren deposit in Uzbekistan to improve their porous structure and adsorption activity. The research will involve the application of thermal activation and alkaline treatment methods to optimize the properties of the coals, which could significantly enhance their effectiveness in various applications, including air and water purification.

EXPERIMENTAL

The objects of the study were BPK and BR grade brown coals, characterized by ash content of 8.6% and 13.6%, respectively. Potassium hydroxide (KOH) of analytical grade was used for chemical activation. During subsequent processing, a 0.5 N hydrochloric acid (HCl) solution was used for neutralization.

For the evaluation of the adsorption properties of the activated carbons, benzene (chemically pure) was chosen as the organic adsorbate to characterize hydrophobic interactions.

The thermal treatment of the samples was carried out in a laboratory setup for pyrolysis and thermoactivation at the “Colloid Chemistry and Industrial Ecology” laboratory of the Institute of General and Inorganic Chemistry of the Academy of Sciences of the Republic of Uzbekistan [16]. The setup includes a sealed reactor with an electric heater, ensuring uniform heating of the raw material to the desired temperature. The reactor operates in an inert gas (argon) atmosphere to prevent oxidation. The raw material is placed on a stainless-steel reaction grid inside the reactor. The process temperature is monitored by a thermocouple connected to the system to maintain stable conditions. The gases released are vented and analyzed, allowing precise control of the gas composition and optimization of the process for obtaining carbon adsorbents.

For chemical activation, the carbonized material, previously obtained by thermal treatment of the coals at 500°C, was mixed with potassium hydroxide (KOH) in different mass ratios (from 1:0.5 to 1:7). The mixing was carried out with thorough agitation to ensure uniform distribution of the activator within the carbon matrix.

After the preparation stage of the mixture, the samples underwent thermal activation at 800°C in an inert gas atmosphere. The heating rate was 10°C/min, and once the target temperature was reached, the samples were held at that temperature for 1 hour. During the activation process, potassium hydroxide (KOH) interacted with the carbon material, leading to the development of a porous structure and an increase in the specific surface area of the coals.

Upon completion of the thermal activation, the carbon materials were treated with a 10% hydrochloric acid (HCl) solution to remove residual alkali and soluble inorganic impurities. Subsequently, the materials were repeatedly washed with distilled water until the filtrate reached a neutral pH, ensuring the complete removal of Cl_2 ions and other residual salts.

The purified carbon materials were dried at 100°C for 1 hour to remove moisture and stabilize the structure. The obtained coals were characterized to assess their textural and adsorption properties.

The particle size analysis of the coals was conducted using the sieve method with a laboratory vibrating sieve SM-300. A 50 g coal sample was sieved through a set of standard sieves with mesh sizes of 1.25, 1.0, 0.5, 0.25, 0.16, and 0.05 mm for 10 minutes at a vibration amplitude of 1.5 mm. After sieving, the residue on each sieve was weighed, and the granulometric composition was then calculated. The obtained data were used to assess the degree of coal grinding and its impact on the adsorption properties.

The method for determining the ash content of carbon adsorbents is based on high-temperature calcination in a muffle furnace. Prior to analysis, the samples were pre-dried at 105°C to a constant weight. A sample of the adsorbent weighing (0.5 ± 0.05) g, ground to a particle size of less than 0.2 mm, was placed in a crucible with a constant weight and evenly distributed.

The muffle furnace was heated to 850°C. The crucible with the sample was placed at the edge of the open furnace and maintained for 3-5 minutes to remove volatile components. Then, the crucible was slowly moved into the zone of constant temperature at a rate not exceeding 2 cm/min, the furnace door was closed, and the calcination was carried out for 15-25 minutes.

After completing the process, the crucible was cooled in a desiccator to room temperature and weighed. The ash content (A_{ad}, %) was calculated using the formula:

$$A_{ad} = \frac{m_1}{m} * 100\%,$$

where m_1 — mass of the residue after calcination, m — mass of the initial sample.

Each measurement was performed 3-5 times. In case of acceptable deviations in the results, the average value was calculated; otherwise, the analysis was repeated. The time for determining the ash content of one sample was 30-45 minutes. The method allowed for the evaluation of the mineral composition of the adsorbents and the effect of modification on their ash content.

Thermogravimetric studies were conducted using a Paulik-Paulik-Erdey system derivatograph. The samples were heated at a rate of 10°C/min with a sample mass of 0.1 g. The derivatograph is equipped with a cell for differential thermal analysis (DTA) and thermobalances for thermogravimetry, recording changes in mass and their rate. The DTA cell includes registrars for the temperature difference between the sample and the reference (aluminum oxide Al_2O_3), as well as the temperature of the sample itself.

The surface morphology was analyzed using scanning electron microscopy (SEM), and the elemental composition of the coals was studied using energy-dispersive spectroscopy (EDS) (Jeol model JSM-21).

To determine the characteristics of the porous structure, such as specific surface area (S), total pore volume (ΣV), and pore diameter (d_{pore}), the method of low-temperature nitrogen adsorption at 77 K was used on a Quantachrome Nova 1000e apparatus. The samples were pre-treated in a vacuum at 100°C for 12 hours. The partial pressure reached 0.995 P/Ps. The adsorption and desorption isotherms of nitrogen were measured in the partial pressure range from 0.005 to 0.995 P/Ps and processed using the BET method. The micropore volume was determined by the t-Plot method, and the mesopore volume by the BJH method. The average pore diameter was estimated using the formula $D_{avg} = 4V/S$. The micropore size distribution, with an average size of 1.15-1.17 nm, was evaluated using the Horvath-Kawazoe (HK) method.

The adsorption isotherms of benzene and water vapors at 20ºC were measured by the gravimetric method on a vacuum adsorption apparatus with McBain-Bakker balances. Data on the setup constructed in the Colloid Chemistry Laboratory (IGIC AS RUz, Academy of Sciences of Uzbekistan) are provided in reference [31]. Before the adsorption measurements, the samples were vacuum-treated at 200 and 500ºC (until the residual pressure in the system reached 10^{-3} mm Hg).

RESULTS AND DISCUSSION

3.1. Thermal analysis of coal samples

Thermal analysis of carbon materials plays a crucial role in evaluating their structure, stability, and functional properties. Studying the thermal behavior allows for the determination of temperature ranges for the decomposition of organic and inorganic components, phase transitions, and the nature of chemical interactions within the samples. Analysis of the thermal decomposition curves also helps to identify the mechanisms of porous structure formation and the extent of volatile component removal, which is critical for the adsorption characteristics of the obtained materials.

1)

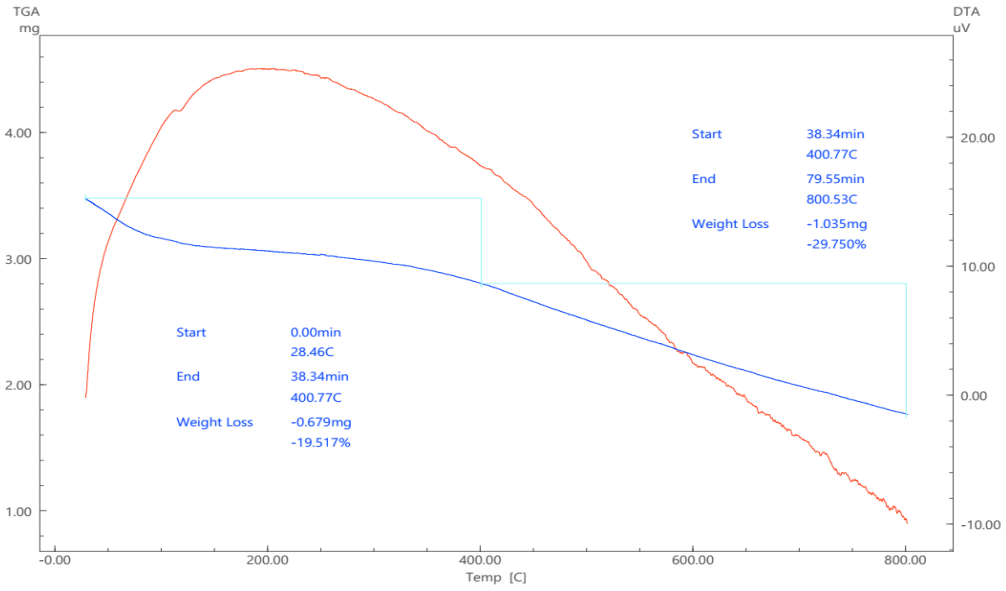

2)

Figure 1. Thermograms of coal samples: 1) BPK; 2) BR.

The thermogram of brown natural coal (BPK) shows three main stages of thermal decomposition, which reflect changes in the sample's mass as a function of temperature. The first stage (27-299°C) is accompanied by a mass loss of approximately 22.86%. This is

associated with the removal of moisture and easily volatile components, which is typical for brown coals with a high content of adsorbed water. The endothermic nature of this process is confirmed by the absence of pronounced exothermic peaks on the DTA curve in this temperature range.

In the second stage (299-559°C), the greatest mass loss is observed, amounting to approximately 43.98%. This stage corresponds to the active thermal decomposition of the coal's organic matrix, including the breakdown of cellulose and lignin-like structures, as well as the release of gaseous products such as CO, CO_2, and hydrocarbons. An exothermic peak is registered on the DTA curve in this range, with a maximum at 471.7°C, indicating an intense oxidation and pyrolysis process of the organic material.

The third stage (559-800°C) is characterized by a further mass loss of 28.93%, which is associated with the combustion of the carbon residue and the residual oxidation of carbon components. In this range, weaker exothermic manifestations are observed, indicating a gradual decrease in the intensity of the reactions.

The thermogram of brown coal BR shows two main stages of thermal decomposition, which allow the characterization of its thermal behavior. The first stage (28-400°C) is accompanied by a mass loss of approximately 19.52%, which is related to the removal of moisture and volatile components. The relatively smaller mass loss compared to brown coal BPK indicates a lower content of moisture and volatile compounds in coal BR. In this temperature range, the DTA curve does not show significant exothermic peaks, indicating that physical processes, such as water evaporation and the release of gaseous volatile substances, dominate.

In the second stage of thermal decomposition, in the temperature range of 400-800°C, the mass loss is approximately 29.75%. This process is associated with the decomposition of the organic matrix of the coal, including pyrolysis and oxidation of carbon components. Compared to brown coal BPK, coal BR shows a smaller mass loss, which indicates a higher content of mineral components and lower reactivity of the organic part.

Overall, BR coal exhibits a lower total mass loss at all stages of thermal decomposition compared to BPK. At the first stage, the difference is 19.52% versus 22.86%, which is explained by the lower moisture and volatile content. At the second stage, the mass loss for BR coal is 29.75% compared to 43.98% for BPK, indicating a lower content of organic matter and higher ash content. These differences are attributed to the composition of the coals, where BR coal contains more mineral inclusions, which reduces its reactivity during heating.

3.2. Change in the mass of coal during thermal and chemical activation

Based on the results of the thermal analysis of BPK and BR lignite coals, preliminary thermal treatment prior to chemical activation was carried out at 500°C. The analysis of thermograms revealed that the main removal of moisture and volatile compounds occurs below 400°C, whereas active decomposition of the organic matrix and the formation of a carbonaceous framework begins in the 400–600°C range. The choice of 500°C as the treatment temperature is justified by the need to eliminate unstable components while preserving a sufficient number of reactive functional groups, thereby enhancing the efficiency of subsequent chemical activation. The duration of thermal treatment at 500°C was set to 2 hours, as the major mass loss occurs within this period, with only a marginal additional decrease (2.5–3.0%) observed thereafter.

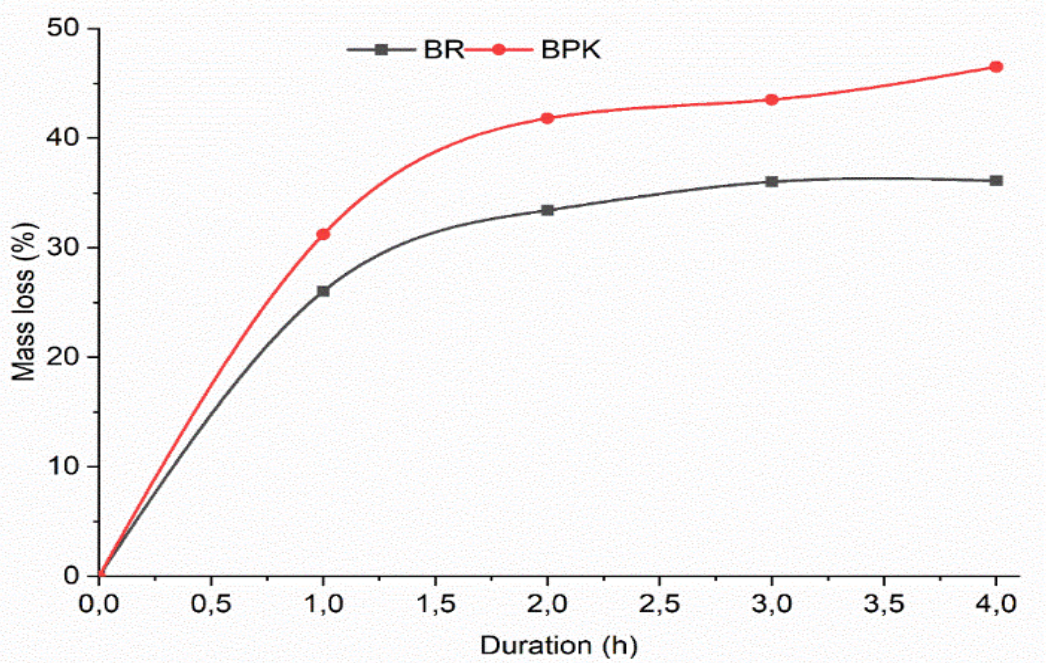

Figure 2. Change in the mass of coal samples during thermal treatment at 500°C.

The analysis of mass loss in BPK and BR coals during thermal treatment at 500°C demonstrated a consistent decrease in mass with increasing treatment time. During the first 2 hours, a significant reduction in mass was observed: 41.8% for BPK coal and 33.4% for BR coal. This intensive mass loss is attributed to the removal of volatile components and degassing of the organic matrix.

At the third hour of thermal treatment, the rate of mass loss significantly decreases, and after 3 hours, the process stabilizes, with minimal changes in the mass of the coals. For BPK coal, the mass loss increases by only 1.7% (up to 43.5%), while for BR coal, it increases by 2.6% (up to 36.0%). At the fourth hour of treatment, the mass loss remains almost unchanged, indicating the completion of the main thermal transformations.

The choice of 2 hours for thermal treatment is based on the optimal balance between mass loss and energy consumption. At this stage, maximum degassing is achieved, along with the preliminary formation of the porous structure, without significant additional energy costs. This ensures the efficient preparation of the coals for subsequent chemical activation.

The study of the influence of the coal:KOH ratio on the yield of carbon materials showed that increasing the amount of activator leads to a decrease in yield due to the intensification of the processes of carbon matrix destruction and the removal of volatile products.

At a ratio of 1:3, the yield of carbon material for BPK was 53.55%, and for BR it was 41.7%, indicating greater resistance of BPK to the action of KOH. Increasing the ratio to 1:5 reduces the yield to 34.1% for BPK and 32.7% for BR, confirming the active etching of the carbon structure.

Further increasing the KOH ratio leads to additional yield reduction: for BPK, the loss is 2.5%, while for BR it is no more than 1.2%. This indicates the differing resistance of the coals to chemical activation. BR coal reaches its degradation limit faster, whereas BPK continues to degrade under higher activator concentration.

3.3. Change in ash content and dispersibility of coals during chemical activation

During the chemical activation of carbon materials, the ash content is an important parameter as mineral impurities can affect the porous structure, mechanical properties, and

adsorption characteristics of coals. The influence of the KOH-to-coal ratio on the ash content of brown coals has been studied. Determining the optimal amount of KOH not only helps to reduce the content of mineral inclusions but also improves the purity of the carbon material, which is particularly important for the subsequent use of activated coals in adsorption processes.

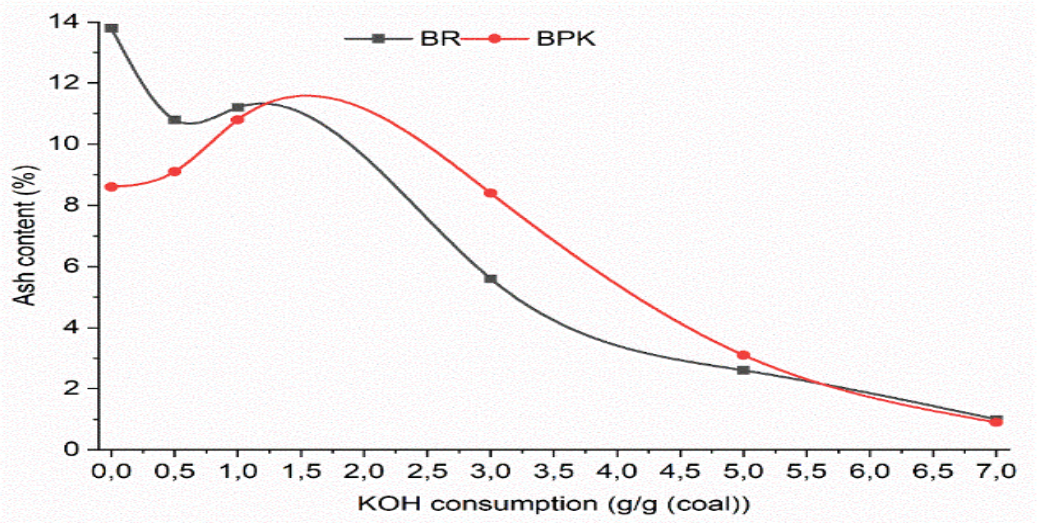

Figure 3. Change in ash content of coals as a function of KOH consumption.

With an increase in the KOH dosage per 1 g of coal, a consistent decrease in ash content is observed for both types of coals. In the initial samples of BR and BPK, the ash content is 13.8% and 8.6%, respectively. During the early stages of activation (0.5-1.0 g of KOH), the ash content changes slightly, which is related to the partial dissolution of mineral impurities. With further increase in the ratio (3-5 g of KOH), the ash content decreases sharply, reaching 5.6% for BR and 8.4% for BPK at a 3:1 ratio. This is due to the active leaching of mineral components during the interaction with KOH. The maximum decrease in ash content (down to 1.0% for BR and 0.9% for BPK) is observed at a 7:1 ratio, which is associated with the almost complete removal of ash impurities and the washing out of most non-carbonaceous compounds. This confirms the high efficiency of KOH as an activating reagent, which promotes the cleaning of the carbon matrix and increases porosity by removing mineral inclusions.

The analysis of the particle size distribution of coals at different stages of processing shows a significant change in the fractional composition of the samples

Table 1.

Dispersed composition of coal samples.

Sample	≥1.25	1.25≥1	1≥0.5	0.5≥0.25	0.25≥0.16	0.16≥0.05	0.05≥
BPK	19	18.1	16.3	17.6	19.3	8.4	1.3
BR	34.6	15.1	13.7	12.7	8.9	14.9	0.1
BPK 500	17.6	14.3	15.9	17.7	13.1	20.3	1.1
BR 500	48.4	14.2	9.7	8.4	10	9.3	
BPK/KOH=1/1	17.6	15.4	18.3	21.2	17.6	9.6	0.3
BR/KOH = 1/1	31.3	13.2	14.8	15.6	9.2	15.3	0.6
BPK/KOH=1/5	2.3	10.8	21.2	15.6	26.8	15.6	7.7
BR/KOH = 1/5	1.7	14.8	19.5	27.2	14.3	16.9	5.6

The initial samples of BPK and BR are characterized by a high proportion of large particles (>1.25 mm), which constitute 19% and 34.6%, respectively. After thermal treatment at 500°C (BPK500 and BR500), an opposite trend is observed: for BPK500, the particle distribution remains relatively uniform, while for BR500, the proportion of larger fractions increases to 48.4%. This may be due to particle agglomeration and an increase in the mechanical strength of the coal.

Chemical activation significantly affects the particle distribution. At a coal: KOH ratio of 1:1, further fragmentation of the structure is observed. The BPK/KOH=1/1 and BR/KOH=1/1 coals show a decrease in the proportion of large particles (>1.25 mm) to 17.6% and 31.3%, respectively, indicating the intensification of structural breakdown processes.

With an increase in the KOH consumption to 1/5, the grinding process becomes more pronounced. The proportion of large fractions (>1.25 mm) decreases to minimal values (2.3% for BPK/KOH=1/5 and 1.7% for BR/KOH=1/5), while the content of fine particles (<0.16 mm) increases, confirming the intensified loosening and etching of the carbon matrix.

Thus, chemical activation leads to significant destruction of the coal structure, especially with an increase in KOH concentration, which promotes the formation of a more dispersed material with an increased specific surface area.

3.4. Change in surface morphology of coal samples during thermal and chemical treatment

The BPK samples (images 1 and 2) demonstrate a chaotic, loose structure with pronounced particle dispersibility. The particle size varies over a wide range, but aggregates with sizes of 10-50 µm predominate. The surface of the particles is unevenly rough, with small pores and fragmented areas, indicating well-developed internal porosity.

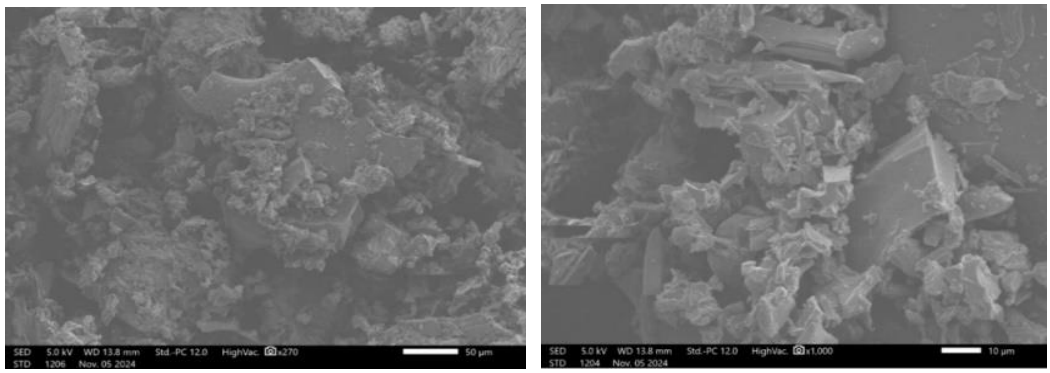

BPK

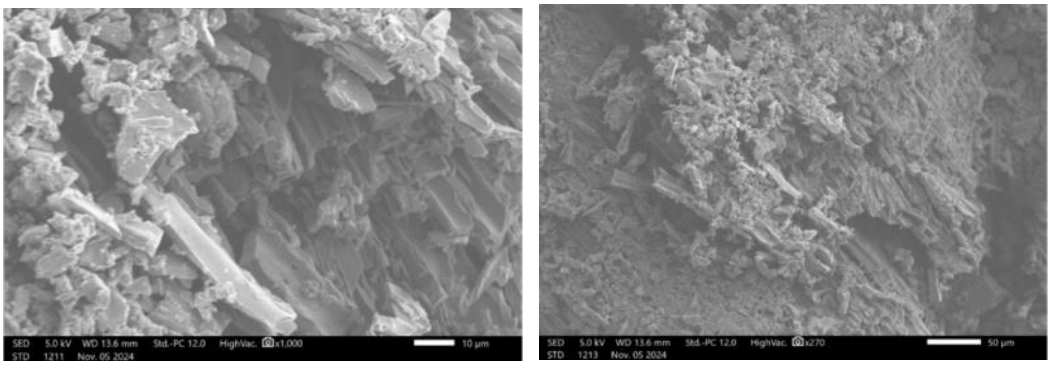

BR

Figure 4. Microscopic images of the original samples.

The image at ×1000 magnification (image 2) shows the presence of pores and fine-dispersed formations, which may indicate a high content of volatile components that contribute to the loosening of the structure during thermal treatment.

The BR samples (images 3 and 4) are characterized by a denser and more layered structure. The particles predominantly have a plate-like shape and a less pronounced dispersion compared to BPK, as seen in the image at ×270 magnification (image 4). In the microphotograph at ×1000 magnification (image 3), the presence of layered fragments can be noted, indicating a more highly structured organization of the carbon material. The particle surface shows a lower number of micropores, suggesting a lesser degree of structural loosening during the processing.

Table 2.

Elemental composition of coal samples.

Sample	C	O	Na	Mg	Al	S	Ca
BR	74.58	23.465	0.090	0.240	0.135	0.195	1.295
BPK	76.20	21.295	0.095	0.335	0.375	0.310	1.525

Elemental analysis of the BR and BPK coals shows that the main components are carbon (C) and oxygen (O). The BPK sample contains more carbon (76.2%) compared to BR (74.6%), indicating a higher degree of carbonization. The oxygen content in BPC is lower (21.3%) compared to BR (23.5%), which may suggest a lower concentration of oxygen-containing functional groups in its structure.

The mineral components, represented by Na, Mg, Al, S, and Ca, are present in small amounts. The highest calcium (Ca) content is recorded in the BPK sample (1.53%), which may be related to a higher concentration of carbonates. Magnesium (Mg) and aluminum (Al) also have higher concentrations in BPK, indicating the possible presence of sample and carbonate impurities.

The sulfur (S) content in both samples is low (0.19-0.31%), indicating a minimal presence of sulfur-containing compounds.

The composition of the ash content of the coals was investigated, and the results are presented in Table 2.

Table 3.

Elemental composition of the ash from coal samples.

Sample	C	O	Na	Mg	Al	Si	S	Ca	Ti	K	Mn
BRK	7,52	48,57	1,86	2,94	9,21	8,24	5,97	14,17	1,15	0,38	
BR	6,35	35,79	2,42	6,08	0,87	0,53	6,03	39,55		1,71	0,67

Analysis of the elemental composition of the ash from the brown coals BPK and BR revealed differences in their mineral composition, which determine their behavior during subsequent processing. The ash from BPK is characterized by a high oxygen content (48.57%) and significant amounts of aluminum (9.21%), silicon (8.24%), and calcium (14.17%), indicating the presence of aluminosilicates and carbonate compounds. The high sulfur content (5.97%) suggests the possible presence of sulfates or pyrite impurities. Sodium (1.86%) and magnesium (2.94%) may be associated with impurities in the raw coal.

The ash from BR contains less oxygen (35.79%) and aluminosilicates (Al – 0.87%, Si – 0.53%) but is characterized by an increased content of calcium (39.55%) and magnesium (6.08%), which confirms the predominance of carbonate compounds. The

elevated concentration of potassium (1.71%) and manganese (0.67%) may indicate the presence of their oxides or carbonates.

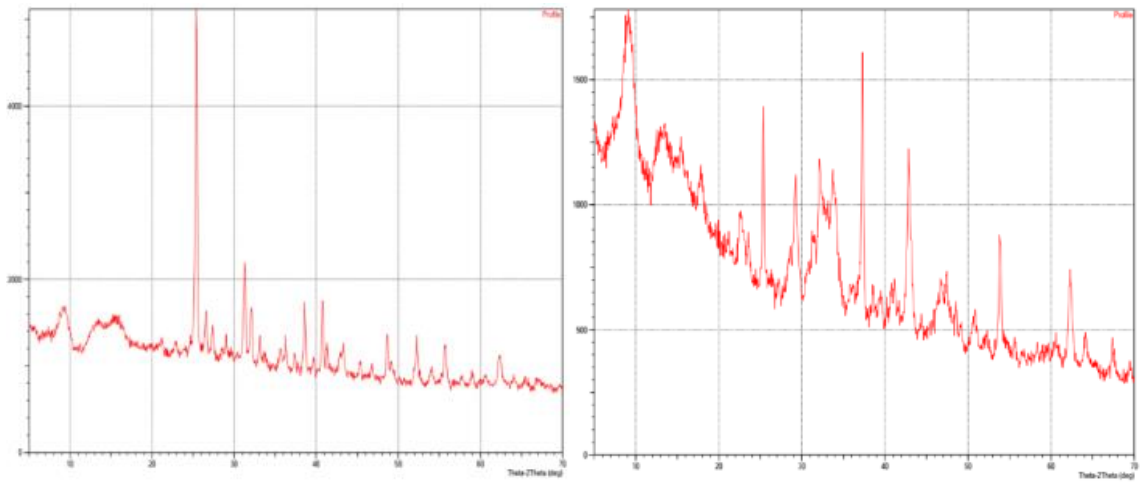

BR **BPK**

Figure 5. X-ray diffractograms of the ash content of the coals.

The X-ray phase analysis of the ash content of the brown coal BPC confirms the presence of several crystalline phases. The most intense peak at 2Θ = 9.19° indicates a significant content of clay minerals, such as kaolinite or montmorillonite. Additional peaks in the range of 2Θ = 13.33°, 15.47°, and 17.96° are also characteristic of aluminosilicate compounds, which aligns with the increased content of aluminum and silicon in the elemental analysis.

The peaks at 2Θ = 22.89° and 25.48° indicate the presence of quartz (SiO_2), which is one of the main components of the ash. In the range of 2Θ = 29.15–32.90°, signals associated with carbonates are observed, specifically calcite ($CaCO_3$) and dolomite.

The presence of aluminosilicates is confirmed by a series of peaks in the range of 2Θ = 37.19° and 42.87°, which may indicate mullite or other silicate compounds. The intense peak at 2Θ = 39.20° could be associated with the presence of hematite (Fe_2O_3) or other iron oxides. The amorphous background in the low-angle region indicates a significant proportion of amorphous phases, which is characteristic of the ash from brown coals.

Thus, the ash of BPK is characterized by a high proportion of aluminosilicates and carbonates, which explains its increased ash content and may influence its reactivity in various processing processes.

The analysis of microscopic images (Fig. 4) of the chemically activated BPK and BR coals allows for the assessment of the impact of activation on morphological characteristics, such as particle size and shape, degree of fragmentation, development of the porous structure, and surface heterogeneity during chemical activation.

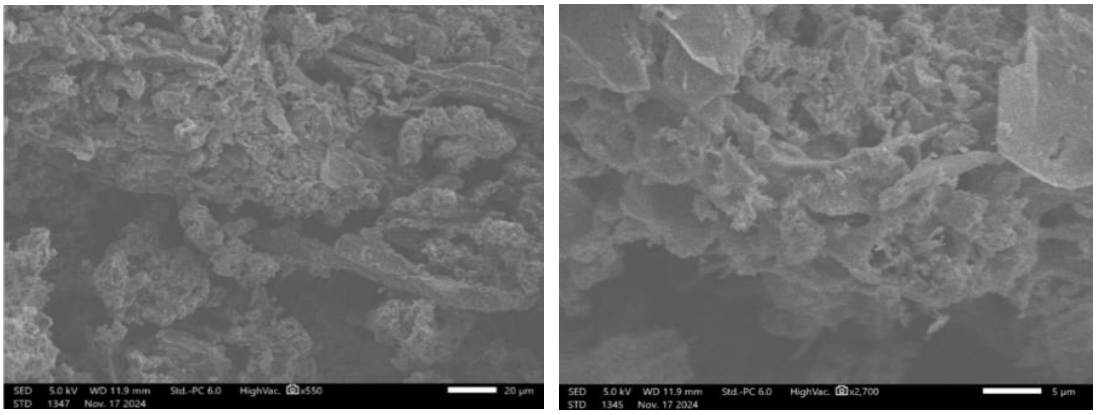

BR/KOH = 1/1

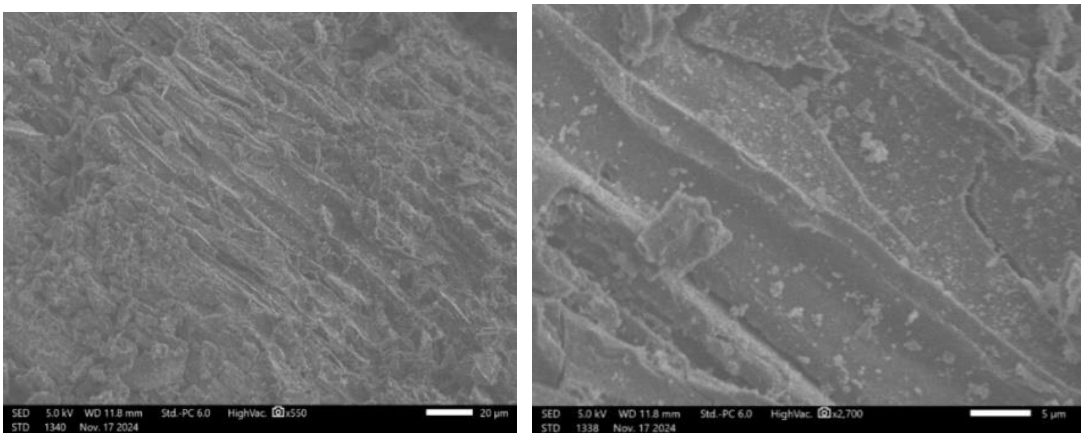

BPK/KOH = 1/1

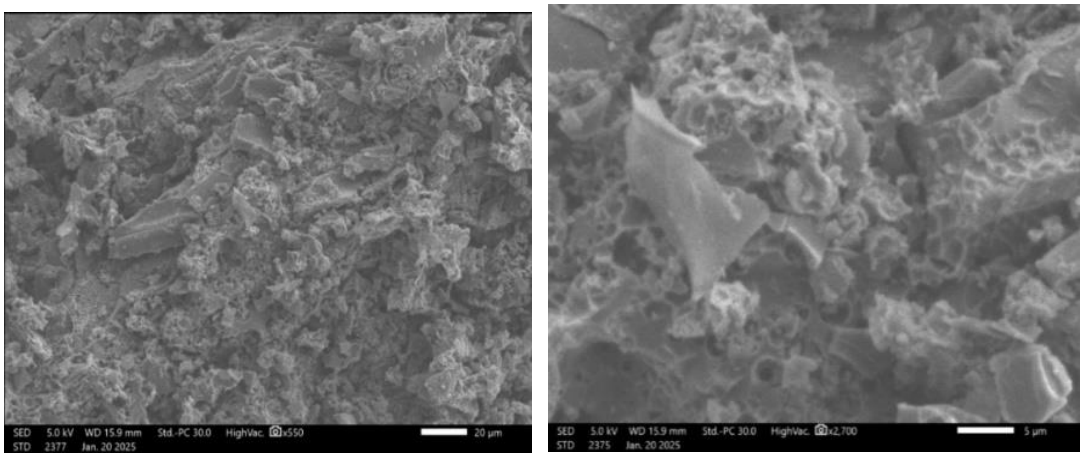

BR/KOH = 1/3

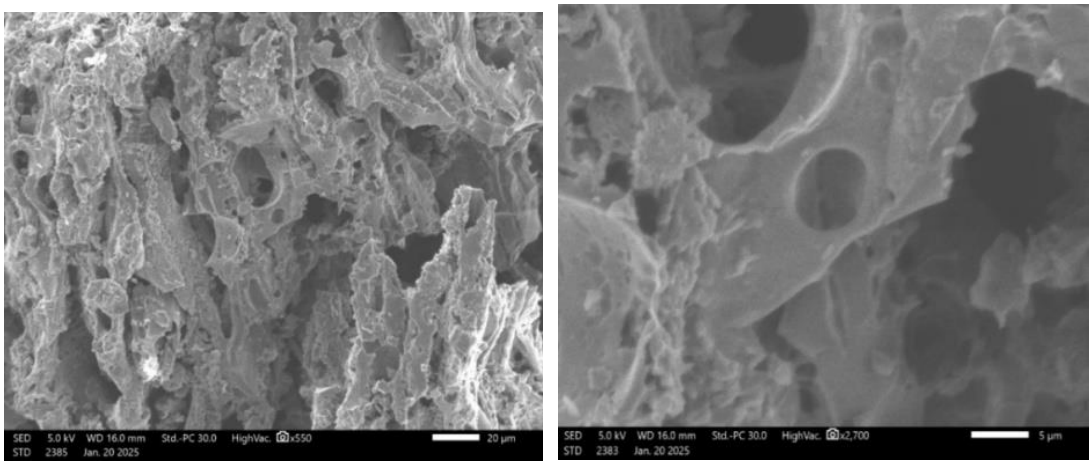

BPK/KOH = 1/3

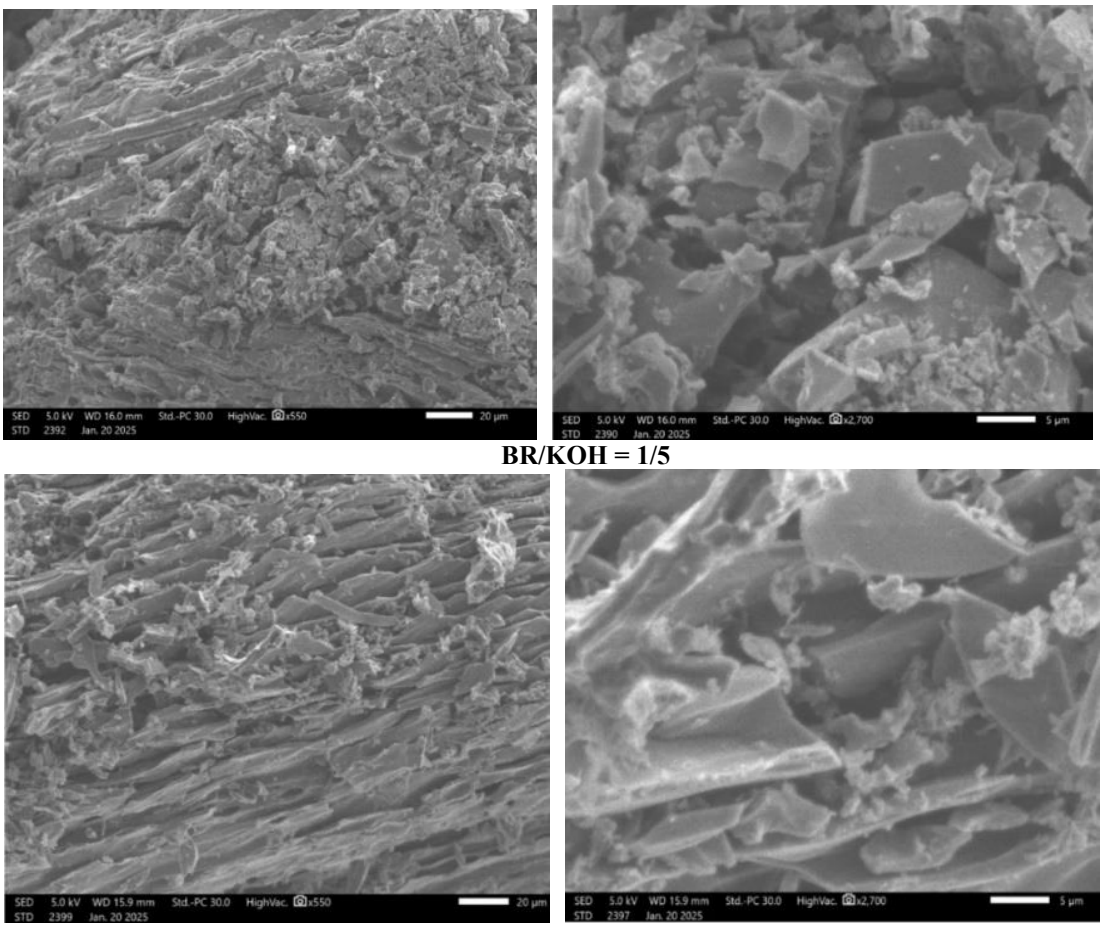

Figure 6. Microscopic images of chemically activated coals.

For the BR/KOH = 1/1 samples, the development of porosity is observed, accompanied by partial structural destruction. At ×550 magnification, a high degree of particle fragmentation is noticeable, indicating intense KOH treatment, which leads to the formation of a branched pore structure and microcracks. At ×2700 magnification, multiple micron-sized pores and loose areas are visible, formed as a result of the selective dissolution of less stable components of the carbon matrix.

The BPK/KOH = 1/1 samples exhibit a more pronounced layered morphology. At ×550 magnification, parallel pore channels are visible, indicating partial preservation of the original texture. At ×2700 magnification, elongated micropores and a network structure are observed, suggesting pore formation primarily through etching along the structural layers of the carbon material.

With the increase in the KOH ratio to 1/3 in the BR/KOH and BPK/KOH samples, further development of the porous structure is observed. The micrographs show the formation of macropores and network channels, indicating active etching of the carbon matrix. The particles become more dispersed, and the surface becomes less homogeneous, suggesting an increase in specific surface area.

At a KOH ratio of 1/5 (BR/KOH = 1/5), the maximum development of the porous structure is observed. Large through channels and an extensive microporous network are formed, as confirmed by the presence of numerous round and elongated pores. The surface acquires a spongy structure with a high degree of loosening, indicating intense interaction with the chemical reagent.

The comparative analysis shows that an increase in the KOH ratio leads to enhanced dissolution of the carbon matrix, promoting the formation of microporous and mesoporous structures. However, at the maximum ratio (1/5), areas of destruction are observed, which may indicate excessive etching.

Further increasing the coal-to-KOH ratio to 1/7 leads to a decrease in the yield of the carbon material and a deterioration in its porous structure. Excessive activation causes intense destruction of the carbon matrix, resulting in the formation of large macropores, a reduction in specific surface area, and a decline in the mechanical strength of the adsorbent.

The micrographs show that with an excess of KOH, the structure becomes excessively loosened, and the pores lose stability. The development of macroporosity is accompanied by an increase in the proportion of fine particles, which negatively affects the mechanical properties of the adsorbent. Additionally, the possible formation of carbonates partially blocks the pores, reducing the accessibility of active sites.

Table 4.

Elemental composition of chemically activated coal samples.

Sample	C	O	Na	Mg	Al	Si	S	Ca	K
BR/KOH=1/1	76,1	22,4	0,1	0,19	0,12	0,13	0,14	0,56	0,26
BR/KOH=1/3	78,9	20,3		0,14	0,11	0,09		0,21	0,24
BR/KOH=1/5	79,4	20,1		0,08	0,1	0,06	0,05		0,21
BR/KOH=1/7	78,6	21,3							0,1
BPK/KOH=1/1	75,3	23,2	0,05	0,23	0,22	0,25		0,48	0,27
BPK/KOH=1/3	77,8	21,8		0,18	0,07	0,06		0,06	0,05
BPK/KOH=1/5	80,5	19,4		0,11	0,04				
BPK/KOH=1/7	79,8	20,1		0,01					0,09

As can be seen from the data in the table, with an increase in the KOH content, the mass fraction of carbon rises, which is related to the removal of non-volatile impurities and the concentration of the carbon phase. Thus, in the BR/KOH samples, carbon increases from 76.1% (1/1) to 79.4% (1/5), and then decreases to 78.6% (1/7), which may be associated with further structural degradation and material loss. A similar trend is observed for the BPK/KOH samples, where the carbon content increases from 75.3% to 80.5% at 1/5, and then decreases to 79.8%.

The oxygen content decreases as the KOH ratio increases to 1/5, indicating partial removal of oxygen-containing functional groups and the formation of a purer carbon structure. However, at 1/7, the oxygen content increases again, which may be associated with the formation of carbonate compounds on the surface.

Mineral components (Na, Mg, Al, Si, S, Ca) are primarily removed at higher KOH ratios, indicating effective leaching. The reduction in calcium and silicon content is particularly noticeable, confirming the destruction of mineral impurities. The potassium content increases in the samples with a higher KOH ratio, which is related to its residual presence after activation.

Thus, the optimal KOH ratio is within the range of 1/3 to 1/5, at which maximum carbon content is achieved, oxygen-containing functional groups are reduced, and undesirable mineral impurities are removed. Further increasing the KOH ratio leads to deterioration of the structure and the possible formation of undesirable compounds, which reduces the activation efficiency.

3.5. Textural characteristics of coal samples based on low-temperature nitrogen adsorption-desorption.

Textural characteristics of carbon materials play a key role in their adsorption properties and determine their effectiveness in various technological processes. One of the most informative methods for studying the structure of porous adsorbents is low-temperature nitrogen adsorption-desorption, which allows for the quantitative assessment of specific surface area, pore volume, and pore size distribution.

The analysis of nitrogen adsorption isotherms allows for the determination of the predominant type of porosity in the studied samples and the identification of the adsorption mechanisms. Based on the shape of the isotherms and their hysteresis loops, conclusions can be made about the presence of micropores, mesopores, or macropores, as well as their interrelationship and degree of development. The pore size distribution is of particular interest, as it affects the accessibility of active sites and the effectiveness of adsorbents in water purification and gas cleaning processes [32-35]. The nitrogen adsorption-desorption isotherms for the studied samples are shown in Fig. 7.

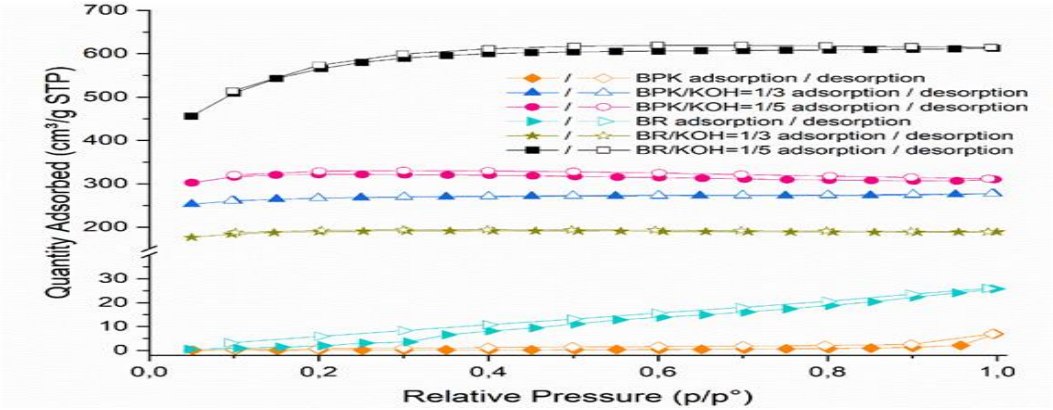

Figure 7. Nitrogen adsorption-desorption isotherms for the samples. (Isotherms in 1).

The adsorption isotherms of the BR sample exhibit the characteristic IV type according to the IUPAC classification for mesoporous materials, with a pronounced hysteresis loop [36]. A significant volume of adsorbed nitrogen in the high relative pressure region (P/Ps > 0.4) indicates the presence of a well-developed mesopore system. The hysteresis loop suggests the presence of pores with a branched structure and capillary condensation within them. Desorption occurs with a noticeable delay, confirming the inhomogeneity of the porous structure and complex mechanisms of adsorbed gas release.

The isotherm of the BPK sample also corresponds to type IV, but with a less pronounced hysteresis loop, indicating a lower degree of development of the porous structure. The volume of adsorbed nitrogen is lower than that of BR, suggesting a smaller specific surface area. The main increase in adsorption occurs at P/Ps > 0.5, which is characteristic of mesoporous materials, but the desorption delay is less pronounced, which may indicate a lower degree of pore branching.

A comparison of the isotherms indicates that BR has a more developed mesoporous structure compared to BPK, which is attributed to its mineral composition and structural features of the carbon matrix. BPK, in turn, exhibits lower sorption capacity.

The analysis of nitrogen adsorption-desorption isotherms for the BR/KOH and BPK/KOH samples at various ratios with the activating agent shows significant development of the porous structure as a result of chemical activation. The isotherms for

BR/KOH = 1/3 and BPK/KOH = 1/3 predominantly exhibit a mesoporous structure. In the low relative pressure region, a moderate increase in the volume of adsorbed gas is observed, indicating the presence of micropores; however, the primary contribution to porosity comes from the mesopore fraction, as confirmed by the increase in adsorption at intermediate P/Ps values. The hysteresis loop is weakly expressed, indicating moderate development of capillary condensation.

With an increase in the KOH ratio to 1/5, a significant rise in specific surface area and total pore volume is observed, which is due to more active modification of the carbon matrix. The isotherms for BR/KOH = 1/5 and BPK/KOH = 1/5 show a sharp increase in adsorption in the initial region, indicating substantial development of microporosity, while the expanded hysteresis loop in the medium and high pressure regions suggests active formation of mesopores. However, the increase in relative pressure during saturation may indicate partial structural degradation at high activating agent consumption.

A comparison of the BR and BPK-based coals shows that the BR/KOH coals have higher sorption capacity and specific surface area compared to the corresponding BPK/KOH samples at the same KOH ratios. This may be due to differences in the initial structure of the coals and their reactivity during activation. Overall, chemical activation leads to the formation of a well-developed porous structure; however, the effectiveness of the process depends on the initial carbon material and activation conditions.

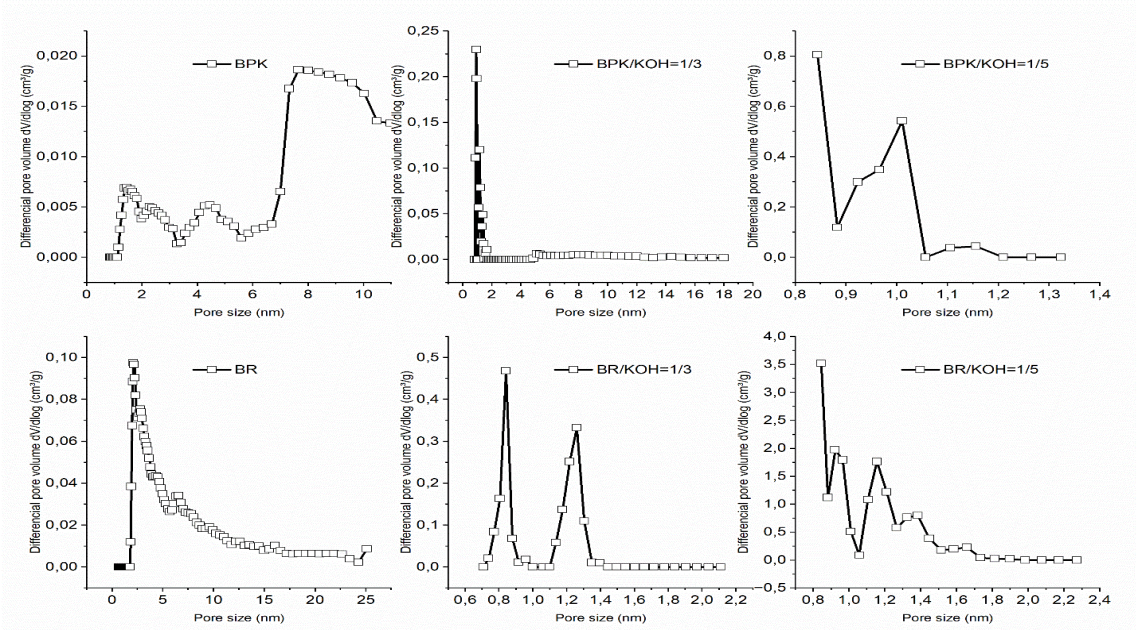

Figure 8. Pore volume distribution by size (all graphs in 1).

The analysis of the pore size distribution for the initial BPC reveals that the majority of the pore volume is concentrated in the range exceeding 20 Å, which indicates a predominantly mesoporous structure of the coal. The maximum contribution to the porosity occurs in the 30–80 Å range, where a distinct peak in the accumulated pore volume is observed. Meanwhile, the pore volume below 20 Å is relatively small, confirming the low content of micropores in the BPK structure.

The pore distribution demonstrates a pronounced unevenness, with several local maxima, indicating the presence of pores of varying sizes. In the range of 80-160 Å, a gradual decrease in pore volume is observed, suggesting less developed macroporosity. Overall, the structure of the BPK is characterized by a predominance of mesopores and a

moderate amount of macropores, which is consistent with nitrogen adsorption data and confirms the limited development of microporosity in the initial material.

The majority of the pore volume of BR is concentrated in the range above 20 Å, similar to the case of BPK. The graph shows a distinct peak in the 30-50 Å range, indicating the dominance of mesopores of this size. Meanwhile, the pore volume in the micropore range (<20 Å) is insignificant. In the 80-160 Å range, the pore volume gradually decreases, but the contribution of macroporous structures remains, distinguishing BR from BPK. Compared to BPK, BR exhibits a more pronounced accumulation of pores in the region up to 50 Å, which may indicate differences in the initial structure of the coals.

The maximum accumulated pore volume is approximately 0.40 cm^3/g for BPK/KOH = 1/3, with the dominant pore sizes in the range up to 10 Å. The greatest contribution to the total pore volume comes from a narrow size interval around 8 Å, indicating the formation of a predominantly microporous structure. In the mesopore range (from 20 Å and above), the pore volume is insignificant. The curve of accumulated pore volume stabilizes after 50 Å. Thus, the coal BPK/KOH = 1/3 demonstrates a pronounced microporosity with limited mesopore development.

In contrast to the original BPK sample, this material demonstrates a significantly higher total pore volume; however, the reduction in the proportion of mesopores may indicate excessive dissolution of the carbon matrix during interaction with KOH. The plateau on the graph of total pore volume suggests that further increases in pore size do not lead to a substantial increase in their contribution to the overall porosity, which is typical for structures with pronounced microporosity.

For BPK/KOH = 1/5, the main pore volume is concentrated in the range of 8-12 Å, with the largest proportion of pores at 8 Å. The total pore volume is approximately 0.46 cm^3/g, which exceeds the corresponding value for the sample with a 1/3 ratio. In contrast to BPK/KOH = 1/3, a slight increase in pores in the 10-12 Å range is observed, which may indicate partial pore expansion due to the higher content of the activating agent. However, the proportion of pores larger than 15 Å remains insignificant, confirming that the material's structure is predominantly microporous.

Compared to the original BR, the activated sample demonstrates a significant increase in pore volume, especially in the micropore region, indicating the high effectiveness of chemical activation in the formation of the porous structure. This is confirmed by the shift of peaks toward smaller sizes and an increase in their intensity, which is characteristic of carbon adsorbents with high sorptive capacity. The analysis of the pore volume distribution by size for BR/KOH = 1/3 shows a significant change in the porous structure compared to the original BR and activated coal BPK/KOH = 1/3. In the BR/KOH = 1/3 sample, the main pore volume is concentrated in the range of 8-12 Å, with the largest proportion of pores at 8 Å, similar to BPK/KOH = 1/3. However, the total pore volume is significantly higher, reaching 0.313 cm^3/g, which notably exceeds the value for the original BR, characterized by a smaller pore volume in the corresponding size range.

Compared to BPK/KOH = 1/3, the BR/KOH = 1/3 sample exhibits more pronounced microporosity, which is attributed to a more intense modification of the carbon matrix under the influence of KOH.

The analysis of the pore volume distribution by size for BR/KOH = 1/5 reveals a further development of the porous structure compared to BR/KOH = 1/3 and the original BR. The majority of the pores are concentrated in the 8–12 Å range, with the maximum peak at 8 Å, similar to BR/KOH = 1/3. However, the total pore volume is significantly higher, reaching 0.96 cm^3/g.

The analysis of the textural characteristics of the coal samples reveals a significant development of the porous structure as a result of chemical activation, accompanied by an

increase in specific surface area and pore volume. The original BPK and BR samples are characterized by low specific surface areas (1.92 and 22.0 m²/g, respectively) and relatively large average pore radii (218.2 and 67.1 Å, respectively). The pore half-width calculated using the DFT model is 23.46 Å for BPK and 21.10 Å for BR, indicating the predominance of a macroporous structure.

Table 5.

Textural Characteristics of the Samples.

Sample	S, m^2/g	*S_1, m^2/g	V_1, sm^3/g	V_2, sm^3/g	**R, Å	Half pore width (DFT)
BPK	1.92	0.57	0.009	0.0035	218.221	23.46
BR	22.0	6.51	0.038	0.007	67.103	21.10
BR/KOH=1/1	310.85	81.2	0.155	0.011	18.5	13.85
BR/KOH=1/3	1027.90	889.95	0.287	0.014	64.156	8.41
BR/KOH=1/5	1371.44	1076.10	0.874	0.017	63.225	8.44
BR/KOH=1/7	1206.72	909.61	0.709	0.015	12.1	8.39
BPK/KOH=1/1	214.5	126.40	0.131	0.016	14.6	20.61
BPK/KOH=1/3	1024.52	819.43	0.384	0.057	80.638	9.23
BPK/KOH=1/5	1001.22	924.24	0.471	0.182	63.859	8.44
BPK/KOH=1/7	708.16	412.51	0.364	0.02	12.6	10.8

** t-Plot Micropore Area; ** Desorption Average Pore Diameter (4V/A by BET)*

After activation with KOH at various ratios, a significant increase in specific surface area is observed. For BR/KOH = 1/1, the specific surface area reaches 310.85 m²/g, accompanied by a decrease in pore radius to 18.5 Å and a reduction in pore half-width to 13.85 Å, indicating the development of a mesoporous structure. With an increase in the KOH ratio to 1/3, a sharp rise in specific surface area to 1027.90 m²/g is observed, along with a substantial decrease in pore half-width to 8.41 Å, suggesting the predominance of micropores. The samples BR/KOH = 1/5 and BR/KOH = 1/7 maintain high specific surface areas (1371.44 and 1206.72 m²/g, respectively) and are characterized by predominantly microporous structures with pore half-widths of approximately 8.4 Å.

A similar trend is observed for the activated BPK samples. At a BPK/KOH ratio of 1/1, the specific surface area increases to 214.5 m²/g, while the average pore radius decreases to 14.6 Å. With further increases in the KOH ratio to 1/3 and 1/5, the specific surface area reaches 1024.52 and 1001.22 m²/g, respectively, and the pore half-width decreases to 9.23 and 8.44 Å, indicating the development of microporosity. However, at a ratio of 1/7, the specific surface area decreases to 708.16 m²/g, and the pore half-width increases to 10.8 Å, which may be attributed to partial structural degradation due to an excessive amount of the activating agent.

A comparison of the activated samples based on BR and BPK shows that BR-derived carbons possess higher sorption capacity and a more developed microporous structure, as evidenced by smaller pore half-widths and larger micropore volumes. In contrast, the BPC-based samples exhibit less pronounced micropore development, which may be attributed to differences in the initial structure of the coals and the activation mechanism.

Thus, the conducted study has demonstrated that altering the conditions of chemical activation allows for targeted control over the porous structure of coal-based samples. Increasing the KOH ratio leads to the development of microporosity, as confirmed by the growth in specific surface area and the reduction of pore half-width to 8.4 Å under optimal conditions. At the same time, excessive concentrations of the activating agent result in partial structural degradation, a decrease in specific surface area, and an increase in pore size. A comparison of the BR- and BPK-based samples revealed that brown coal (BR) is more prone to micropore development, whereas BPC-derived coals retain a significant

proportion of mesopores. These findings enable the prediction of the sorption properties of the resulting materials and the purposeful modification of their structure according to specific application requirements.

3.6. Adsorption activity for benzene from the gas phase

The adsorptive activity of carbon materials for benzene from the gas phase is an important indicator of their textural characteristics and ability to retain organic compounds. Benzene, as a model organic compound, is widely used to evaluate the sorptive capacity of porous materials, as its molecules exhibit high mobility and can adsorb both in micropores and mesopores [37].

The determination of benzene vapor adsorption allows for the characterization of surface area, pore volume, and pore distribution, as well as the identification of structural changes in carbon adsorbents after thermal and chemical treatment [38]. The obtained data enable the evaluation of how coal modification affects their sorptive properties and help determine the optimal activation conditions for producing materials with high efficiency in removing organic pollutants from the gas phase.

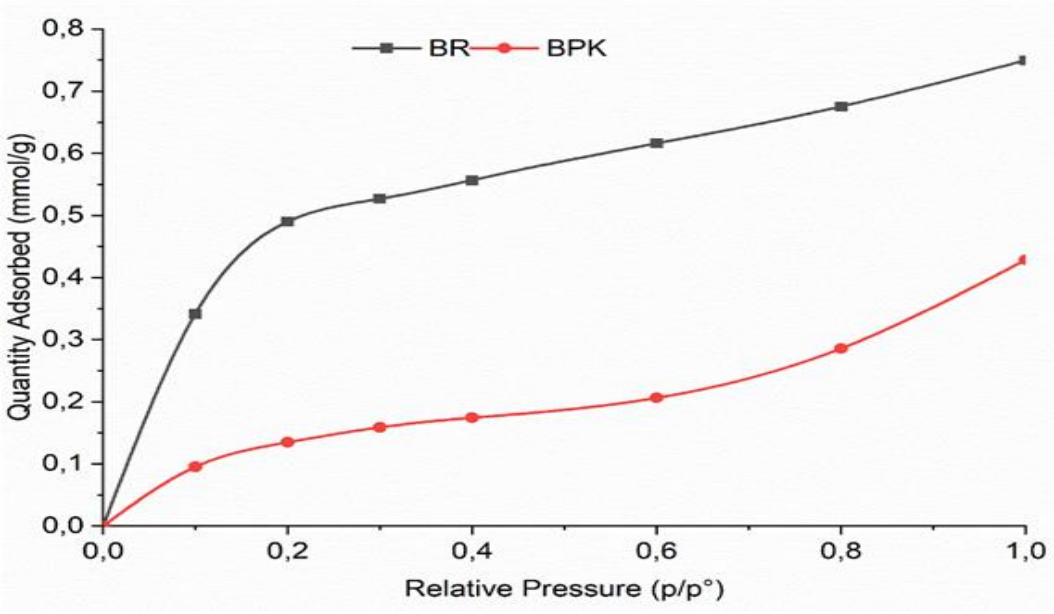

Figure 9. Adsorption isotherms of benzene vapors on the original coal samples.

The analysis of benzene vapor adsorption isotherms on the original BPK and BR coal samples allows for the characterization of their textural properties and the features of their porous structure.

The isotherms of both samples exhibit characteristic features of microporous materials. For the BR coal, a significantly higher adsorption capacity is observed, as confirmed by the limiting adsorption value (A_0) of 0.350 mmol/g, whereas for the BPK, this value is only 0.106 mmol/g.

In benzene adsorption on activated carbons, not only micropores play a key role, but mesopores and the characteristics of the carbon matrix surface are also of significant importance. Although benzene molecules are small enough to effectively fill micropores less than 2 nm (20 Å) in size, their adsorption on the studied samples is governed not only by capillary effects in narrow pores but also by interactions with active surface sites, as well as the possibility of diffusion through the mesoporous system.

The surface area (S), calculated from adsorption data, is 84.24 m^2/g for BR and 25.53 m^2/g for BPK, indicating a significant development of texture in BR. The micropore

volume (V_1) for BR is higher (0.059 cm^3/g) compared to BPK (0.023 cm^3/g), confirming the greater capacity of the microporous structure. However, the mesopore volume (V_2) is higher for BPK (0.015 cm^3/g vs. 0.007 cm^3/g for BR), which may indicate a more developed mesoporous system in this coal.

Table 6.

Data on the porous structure from the adsorption of benzene vapors.

Sample	A_0, mmol/g	S, m^2/g	V_1, sm^3/g	V_2, sm^3/g	R, Å
BPK	0.106	25.53	0.023	0.015	29.9
BR	0.350	84.24	0.059	0.007	15.8
BR/KOH=1/1	1.291	310.85	0.185	0.011	18.5
BR/KOH=1/3	2.008	483.49	0.287	0.014	12.4
BR/KOH=1/5	6.283	1513.04	0.904	0.017	11.9
BR/KOH=1/7	5.011	1206.72	0.712	0.015	12.1
BPK/KOH=1/1	2.330	561.06	0.331	0.02	14.6
BPK/KOH=1/3	2.784	670.38	0.392	0.017	12.2
BPK/KOH=1/5	2.826	680.39	0.407	0.019	12.4
BPK/KOH=1/7	2.526	608.16	0.364	0.02	12.6

The pore radius (RR) for BPC is 29.9 Å, whereas for BR it is significantly smaller at 15.8 Å. This indicates that BPK is characterized by a broader porous structure, while BR predominantly has narrow micropores.

The difference in specific surface area and benzene adsorption activity between the original BR and BPK coals is due to their structural and chemical characteristics. Although the specific surface area of BR (22.0 m^2/g) is more than 11 times higher than that of BPK (1.92 m^2/g), the sorption capacity for benzene is only 3.3 times higher (0.350 vs. 0.106 mmol/g). This is because BR contains not only micropores but also mesopores, which facilitate the effective diffusion of benzene and enhance its adsorption, despite the moderate specific surface area values.

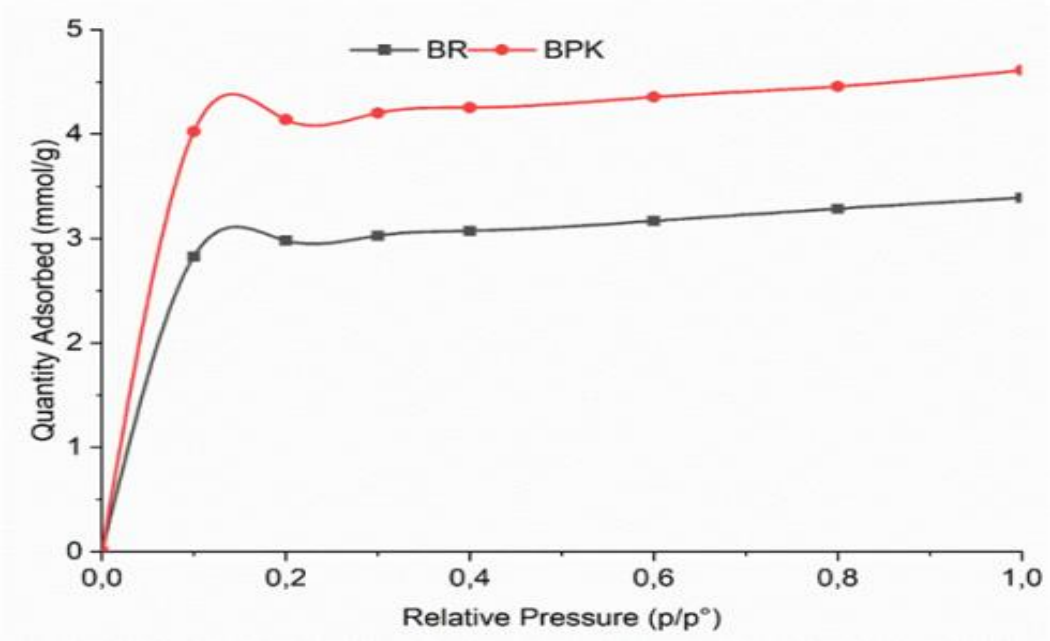

Figure 10. Adsorption isotherms of benzene vapors on chemically activated coal samples at a coal/KOH ratio of 1/3.

Pore distribution also plays a key role: the pore radius in BR is 15.8 Å, compared to 29.9 Å in BPK, which favors capillary condensation and the retention of benzene

molecules. In BPK, wide pores dominate, which are less effective for adsorption, limiting its sorptive characteristics.

Additionally, the chemical nature of the surface affects the interaction with benzene. The higher degree of graphitization in BR makes its surface hydrophobic, promoting the effective retention of nonpolar molecules. In contrast, BPK, with oxygen-containing functional groups, demonstrates a lower affinity for benzene.

The analysis of benzene vapor adsorption isotherms on chemically activated BR/KOH=1/1 and BR/KOH=1/3 coals shows a significant increase in adsorption capacity compared to the original samples. The adsorption isotherms exhibit a rapid increase in adsorption at low relative pressures (P/Ps < 0.1), which is characteristic of microporous materials with high sorptive capacity.

The BPK/KOH=1/3 sample has a higher specific surface area (670.38 m^2/g) and adsorption capacity (2.784 mmol/g) compared to BR/KOH=1/3 (483.49 m^2/g and 2.008 mmol/g, respectively). This indicates a more intense etching of the carbon matrix in BPK during activation, which promotes the formation of a well-developed porous structure. The micropore volume in the BPK/KOH=1/3 sample is 0.392 sm^3/g, which is higher than in BR/KOH=1/3 (0.287 sm^3/g), confirming the predominant development of microporosity.

The average pore radius for both samples is similar, ranging from 12.2 to 12.4 Å, indicating the formation of micropores around 1.2 nm in size, which effectively facilitate benzene adsorption. The mesopore volume (V_2) in both samples remains low (0.017 and 0.014 sm^3/g), confirming the predominant development of a microporous structure.

The higher values of A_0 and S for the BPK/KOH=1/3 sample confirm that chemical activation of BPK at this activator ratio promotes the formation of a more developed porous structure, making this material more promising for benzene vapor adsorption.

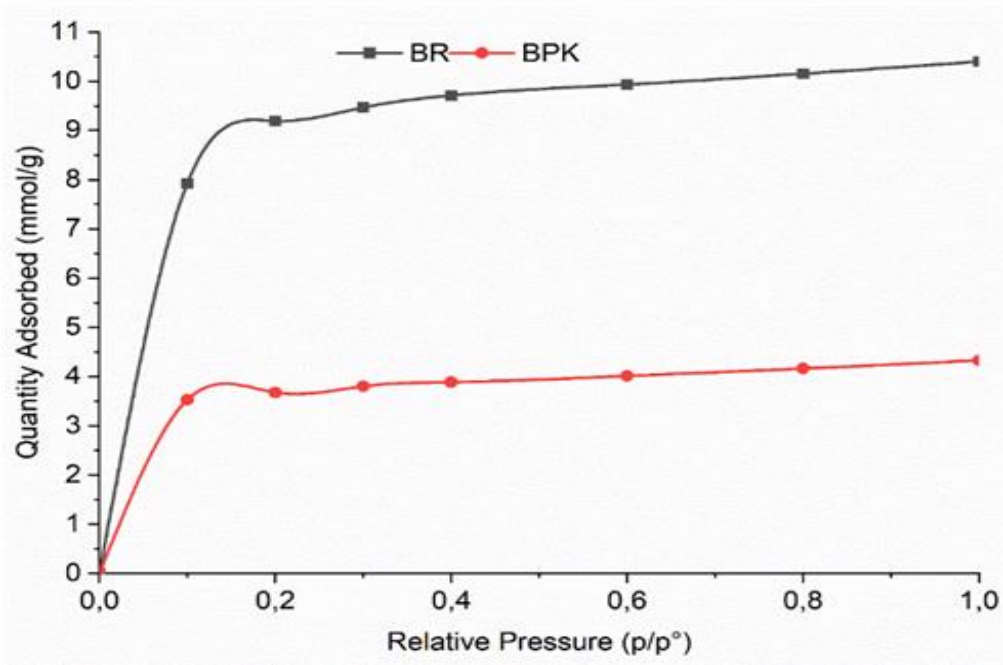

Figure 11. Adsorption isotherms of benzene vapors on chemically activated coal samples at a coal/KOH ratio of 1/5.

The BR/KOH=1/5 coals exhibit the highest specific surface area (1513.04 m^2/g) and adsorption capacity (6.283 mmol/g), which is associated with active changes in the carbon matrix and the formation of a well-developed microporous structure. The micropore

volume (0.904 cm^3/g) in this sample is also the highest among all the coals studied. However, with further increasing the KOH ratio to 1/7, there is a decrease in specific surface area to 1206.72 m^2/g and adsorption capacity to 5.011 mmol/g, which may be due to excessive destruction of the carbon framework and pore merging [39].

A similar trend is observed for BPK-based coals: as the KOH ratio increases to 1/5, the specific surface area increases to 680.39 m^2/g, and the adsorption capacity rises to 2.826 mmol/g. However, further increasing the activator amount to 1/7 leads to a decrease in these parameters (608.16 m^2/g and 2.526 mmol/g, respectively), indicating partial degradation of the material's structure.

The average pore radius in the BR/KOH=1/5 and BR/KOH=1/7 samples ranges from 11.9 to 12.1 Å. In contrast, the pore radius in the BPK/KOH=1/5 and BPK/KOH=1/7 samples is slightly larger (12.4 to 12.6 Å), indicating a less dense structure of the carbon material. Meanwhile, the micropore volume in the BR/KOH=1/5 coals (0.904 sm^3/g) is almost twice as high as in the BPK/KOH=1/5 coals (0.407 sm^3/g), which explains the higher adsorption capacity of the former.

The difference in benzene adsorption capacity between activated coals based on BPK and BR, particularly at high KOH ratios (1/5 and 1/7), is related to several key factors, including the morphology of the porous structure, the pore size distribution, and the chemical properties of the carbon matrix.

Firstly, activated coals based on BR demonstrate higher benzene adsorption capacities (6.283 mmol/g at BR/KOH=1/5 and 5.011 mmol/g at BR/KOH=1/7) compared to similar samples based on BPK (2.826 mmol/g and 2.526 mmol/g, respectively). This indicates that after activation, BR retains a more developed system of narrow mesopores and wide micropores, which provides optimal conditions for benzene retention through capillary condensation and a high density of sorption centers.

Secondly, the differences in pore size distribution have a significant impact. In BPK-based coals, even after chemical activation, a higher proportion of wide mesopores and macropores remains, making them less efficient for benzene adsorption. In contrast, BR-based coals with KOH ratios of 1/5 and 1/7 form a more balanced porous structure, including well-developed micropores (8–12 Å), which are critical for effective adsorption of benzene molecules. Meanwhile, BPK/KOH=1/5 and 1/7 have a slightly larger average pore radius (12.4–12.6 Å), which can reduce the adsorption capacity due to diminished specific interactions between benzene and the carbon matrix.

Another important factor is the differences in the chemical composition of the carbon matrix. The brown coal BPK, in its original state, contains a higher number of oxygen-containing functional groups, which, after chemical activation, may partially preserve polar regions on the surface. These groups do not facilitate effective interaction with benzene, which is a nonpolar molecule. In the case of BR, activation leads to a higher degree of graphitization on the surface, making it more hydrophobic and, consequently, more prone to benzene adsorption.

Thus, the decrease in adsorption activity for BPK/KOH=1/5 and 1/7 compared to BR/KOH=1/5 and 1/7 is due to the less developed microporous structure, lower density of sorption centers in the optimal pore size range, and the potential presence of residual oxygen-containing groups, which reduce the hydrophobicity of the surface.

CONCLUSION

In this work, a study of brown coals of the BPK and BR grades was conducted, including thermal analysis, examination of the mass change of the coals during thermal and chemical activation, changes in ash content and dispersibility, morphological

characteristics of the surface, texture properties based on low-temperature nitrogen adsorption-desorption, and adsorption activity towards benzene.

The results of the thermal analysis showed that the degradation of the carbon matrix and mass loss occur in several stages, with the most intense mass reduction observed in the range of 300–600°C, which is associated with the removal of volatile substances and the destruction of the organic structure. The introduction of chemical activation using KOH leads to additional etching of the carbon matrix, accompanied by an increase in the yield of gaseous and liquid products.

The change in the mass of the coals during chemical activation confirms the significant impact of the activating agent on the material's structure. As the KOH ratio increases, a more pronounced removal of unstable components occurs, leading to a reduction in the mass of the solid residue. However, at ratios of 1/5 and higher, a decrease in the yield of the final product is observed, indicating the destruction of the coal structure and excessive dissolution of the carbon matrix.

The analysis of ash content showed that with an increase in the amount of KOH, the mineral impurities decrease, which is associated with the leaching of inorganic compounds during the activation process. At a KOH ratio of 1/5, the minimum ash content values are reached, confirming the effectiveness of the chemical treatment in removing mineral inclusions. The change in the dispersibility of the coals demonstrates a reduction in the larger fractions and an increase in the proportion of finer particles, which is due to the destruction of the carbon skeleton under the action of the activator.

The morphological analysis of the coal surface before and after activation revealed significant changes in the structure. The initial samples exhibit a dense and weakly porous surface, while after treatment with KOH, developed pore systems of varying morphology are formed. At low KOH ratios (1/1–1/3), the structure remains relatively intact, but at a ratio of 1/5 and higher, significant destruction is observed, with the formation of mesh-like structures and expansion of the pore space.

The analysis of texture characteristics showed that with an increase in the amount of KOH, the development of the porous structure is significantly enhanced. While the initial BPK and BR coals have low specific surface areas (1.92 and 22.0 m^2/g, respectively), chemical activation increases the specific surface area by orders of magnitude, reaching maximum values of 1371.4 m^2/g (BR/KOH=1/5) and 1024.5 m^2/g (BPK/KOH=1/3). At the same time, the pore distribution changes: in the activated coals, micropores (7–12 Å) predominate, which is associated with the selective leaching of less stable structural fragments of the carbon matrix. However, at high KOH ratios, pore expansion occurs, which may lead to a decrease in adsorption capacity due to excessive carbon dissolution.

Thus, the conducted study showed that chemical activation leads to a significant increase in specific surface area and the development of a porous structure, which directly affects the adsorption properties for benzene. Optimal activation conditions are achieved at KOH ratios of 1/3–1/5, where a developed microporous structure is formed, providing maximum adsorption capacity. At the same time, excessive increase in KOH consumption can lead to a decrease in structural integrity and a reduction in sorption efficiency, which should be considered when developing adsorbents based on brown coals.

REFERENCES

1. Ahmed, M., Mavukkandy, M.O., Hasan, S.W., 2022. Recent developments in hazardous pollutants removal from wastewater and water reuse within a circular economy. npj Clean Water. doi:10.1038/s41545-022-00154-5.
2. Wójtowicz, B.; Kordyzon, M.; Bąk-badowska, J.; Gregorczyk, M.; Gworek, B.; Żeber-Dzikowska, I. 2022. Chemicals in wastewater and sewage sludge—An underestimated

health and environmental threat. J. Elem., 27, 847–859. https://doi.org/10.5601/jelem.2022.27.3.2283.
3. González, S.O.; Almeida, C.A.; Calderón, M.; Mallea, M.A.; González, P. 2014. Assessment of the water self-purification capacity on a river affected by organic pollution: Application of chemometrics in spatial and temporal variations. Environ. Sci. Pollut Res., 21, 10583–10593. https://doi.org/10.1007/s11356-014-3098-y.
4. Tanasa, I.; Cazacu, M.; Sluser, B. 2023. Air Quality Integrated Assessment: Environmental Impacts, Risks and Human Health Hazards. Appl. Sci., 13, 1222. https://doi.org/10.3390/app13021222.
5. Glencross, D.A.; Ho, T.R.; Camiña, N.; Hawrylowicz, C.M.; Pfeffer, P.E. 2020. Air pollution and its effects on the immune system. Free Radical Biol. Med., 151, 56–68. https://doi.org/10.1016/j.freeradbiomed.2020.01.179.
6. T. T. Lim and X. Huang, 2007. Evaluation of kapok (Ceiba pentandra (L.) Gaertn.) as a natural hollow hydrophobic-oleophilic fibrous sorbent for oil spill cleanup, Chemosphere, vol. 66, no. 5, pp. 955–963, .https://doi.org/10.1016/j.chemosphere.2006.05.062.
7. D. Wang, T. Silbaugh, R. Pfeffer, and Y. S. Lin, 2010. Removal of emulsified oil from water by inverse fluidization of hydrophobic aerogels, Powder Technol., vol. 203, no. 2, pp. 298-309, https://doi.org/10.1016/j.powtec.2010.05.021.
8. B. I. Waisi, J. T. Arena, N. E. Benes, A. Nijmeijer, and J. R. McCutcheon, 2019. Activated carbon nanofiber nonwoven for removal of emulsified oil from water, Microporous Mesoporous Mater., vol. 296, no. October, p. 109966, 2020. https://doi.org/10.1016/j.micromeso.2019.109966.
9. F. Al Jabri, L. Muruganandam, and D. A. D. A. Aljuboury. 2019. Treatment of the oilfield-produced water and oil refinery wastewater by using inverse fluidization - A review, Glob. Nest J., vol. 21, no. 2, pp. 204–210. https://doi.org/10.30955/gnj.002975.
10. S. Syed, M. I. Alhazzaa, and M. Asif, 2011. Treatment of oily water using hydrophobic nano-silica, Chem. Eng. J., vol. 167, no. 1, pp. 99–103, https://doi.org/10.1016/j.cej.2010.12.006.
11. Lokteva, E.S.; Golubina, E.V. 2019. Metal-support interactions in the design of heterogeneous catalysts for redox processes. Pure Appl. Chem., 91, 609–631. https://doi.org/10.1016/j.cej.2010.12.006.
12. Nowicki, P.; Gruszczyńska, K.; Urban, T.; Wiśniewska, M. 2022. Activated biocarbons obtained from post-fermentation residue as potential adsorbents of organic pollutants from the liquid phase. Physicochem. Probl. Miner. Process., 58, 146357. https://doi.org/10.37190/ppmp/146357.
13. Koul, B.; Yakoob, M.; Shah, M.P. 2022. Agricultural waste management strategies for environmental sustainability. Environ. Res., 206, 112285. https://doi.org/10.1016/j.envres.2021.112285.
14. Olatunji, K.O.; Ahmed, N.A.; Ogunkunle, O. 2021. Optimization of biogas yield from lignocellulosic materials with different pretreatment methods: A review. Biotechnol. Biofuels., 14, 159. https://doi.org/10.1186/s13068-021-02012-x.
15. Saleem, J., Shahid, U., Hijab, M., Mackey, H., McKay, G. 2019. Production and applications of activated carbons as adsorbents from olive stones. Biomass Conv. Bioref., 9, 775–802. https://doi.org/10.1007/s13399-019-00473-7.
16. Bicil, Z., Dogan, M. 2021. Characterization of activated carbons prepared from almond shells and their hydrogen storage properties. Energy Fuels. 35, 10227–10240. https://doi.org/10.1021/acs.energyfuels.1c00795.

17. Oladimeji, T.E., Odunoye, B.O., Elehinafe, F.B., Obanla, O.R., Odunlami, O.A. 2021. Production of activated carbon from sawdust and its efficiency in the treatment of sewage water. Heliyon 7, e05960. https://doi.org/10.1016/j.heliyon.2021.e05960.
18. Jedynak, K., Charmas, B. 2021. Preparation and characterization of physicochemical properties of spruce cone biochars activated by CO_2. Materials, 14, 3859. https://doi.org/10.3390/ma14143859.
19. Shafeeyan, M. S., Daud, W. M. A. W., Houshmand, A., & Shamiri, A. 2010. A review on surface modification of activated carbon for carbon dioxide adsorption. Journal of Analytical and Applied Pyrolysis. https://doi.org/10.1016/j.jaap.2010.07.006.
20. Herawan, S. G., Ahmad, M. A., Putra, A., & Yusof, A. A. 2013. Effect of CO_2 flow rate on the pinang frond-based activated carbon for methylene blue removal. The Scientific World Journal, https://doi.org/10.1155/2013/545948.
21. Hesas, R. H., Arami-Niya, A., Wan Daud, W. M. A., & Sahu, J. N. 2013. Preparation and characterization of activated carbon from apple waste by microwave-assisted phosphoric acid activation: Application in methylene blue adsorption. BioResources, 8(2), 2950–2966. https://doi.org/10.15376/biores.8.2.2950-2966.
22. Tan, I. A. W., Ahmad, A. L., & Hameed, B. H. 2008. Optimization of preparation conditions for activated carbons from coconut husk using response surface methodology. Chemical Engineering Journal, 137(3), 462–470. https://doi.org/10.1016/j.cej.2007.04.031
23. Yang K, Peng J, Srinivasakannan C, Zhang L, Xia H and Duan X 2010. Preparation of high surface area activated carbon from coconut shells using microwave heating. Bioresour. Technol. 101 (15) 6163-6169. https://doi.org/10.1016/j.biortech.2010.03.001.
24. Wang J and Kaskel S. 2012. KOH activation of carbon-based materials for energy storage J. Mater. Chem. 22 (45) 23710-23725. https://doi.org/10.1039/c2jm34066f.
25. Paryanto, Wibowo, W. A., Hantoko, D., & Saputro, M. E. 2019. Preparation of Activated Carbon from Mangrove Waste by KOH Chemical Activation. In IOP Conference Series: Materials Science and Engineering. Institute of Physics Publishing., Vol. 543. https://doi.org/10.1088/1757-899X/543/1/012087
26. Srinivasakannan, C., Abu Bakar, Z. 2004. Production of activated carbon from rubber wood sawdust. Biomass and Bioenergy, 27(1), 89–96. https://doi.org/10.1016/j.biombioe.2003.11.002
27. Seitnazarova O., Kalbaev A., Mamataliev N., Abdikamalova A., Najimova N., 2025. Structural features of montmorillonite-surfactant systems: influence of surfactant packing density
and montmorillonite surface nature. Journal of Chemical Technology and Metallurgy, 60, 1, 43-62. https://doi.org/10.59957/jctm.v60.i1.2025.5
28. Guy, P. J., Perry, G. J. 1992. Victorian brown coal as a source of industrial carbons: a review. Fuel. https://doi.org/10.1016/0016-2361(92)90088-6
29. Amarasekera, G., Scarlett, M. J., & Mainwaring, D. E. 1998, Development of microporosity in carbons derived from alkali digested coal. Carbon, 36(7–8), 1071–1078. https://doi.org/10.1016/S0008-6223(98)00079-7.
30. Lillo-Ródenas, M. A., Cazorla-Amorós, D., & Linares-Solano, A. 2003. Understanding chemical reactions between carbons and NaOH and KOH: An insight into the chemical activation mechanism. Carbon, 41(2), 267–275. https://doi.org/10.1016/S0008-6223(02)00279-8.
31. Khoshimov Sh., Raxmonaliyeva N., Askarova D., Seytnazarova O., Abdikamalova A. 2024. Changes in the porous structure of carbonizate of carbon containing raw under

alkaline activation. AIP Conf. Pro. 11 March; 3045 (1): 030059. https://doi.org/10.1063/5.0197789.
32. Shendrik, T. G., Tamarkina, Y. V., Khabarova, T. V., Kucherenko, V. A., Chesnokov, N. V., & Kuznetsov, B. N. 2009. Formation of the pore structure of brown coal upon thermolysis with potassium hydroxide. Solid Fuel Chemistry, 43(5), 309–313. https://doi.org/10.3103/S0361521909050097.
33. Tamarkina, Y. V., Kolobrodov, V. G., Shendrik, T. G., Kucherenko, V. A. 2009. Properties of adsorbents prepared by the alkali activation of Aleksandriisk brown coal. Solid Fuel Chemistry, 43(4), 233–237. https://doi.org/10.3103/S0361521909040090
34. Tamarkina, Y. V., Kucherenko, V. A., Shendrik, T. G. 2015. Interrelation of gas generation and pore formation on the alkaline activation of brown coal. Solid Fuel Chemistry, 49(2), 91–98. https://doi.org/10.3103/S036152191502010X.
35. Tamarkina, Y. V., Kucherenko, V. A., & Shendrik, T. G. 2012. Nanoporous brown coal adsorbents prepared by alkaline activation with thermal shock. Solid Fuel Chemistry, 46(5), 289–294. https://doi.org/10.3103/S0361521912050114
36. Thommes, M., Kaneko, K., Neimark, A.V., Olivier, J.P., Rodriguez-Reinoso, F., Rouquerol, J., & Sing, K.S.W. 2015. Physisorption of gases, with special reference to the evaluation of surface area and pore size distribution (IUPAC Technical Report). Pure and Applied Chemistry, 87(9-10), 1051–1069. https://doi.org/10.1515/pac-2014-1117.
37. Salehi R., Dadashian F., Abedi M., Eliassi A. 2025. Adsorption studies of benzene and toluene in gas phase onto activated carbon fabrics in fixed bed column. Heliyon. 11(2). doi:10.1016/j.heliyon.2025.e42071.
38. Mamataliev, N., Abdikamalova, A., ... Eshmetov, I., 2025. The role of hydrocarbon radicals in the formation of structural and adsorption characteristics of the montmorillonite–surfactant system. Adsorption Science and Technology 43. doi:10.1177/02636174251377860.
39. Nandi R., Jha M.K., Guchhait S.K., Sutradhar D., Yadav S. 2023. Impact of KOH activation on rice husk derived porous activated carbon for carbon capture at flue gas alike temperatures with high CO_2/N_2 selectivity // ACS Omega. 8(5). DOI: 10.1021/acsomega.2c06955.